GEOPHYSICAL RESEARCH LETTERS, VOL. 20, NO. 9, PAGES 767-770, MAY 5, 1993

PARTICLE TRACING IN THE MAGNETOSPHERE: NEW ALGORITHMS AND RESULTS

R. B. Sheldon and J. D. Gaffey, Jr.

University of Maryland, College Park, Maryland

We use a fast, efficient method to trace charged particles through realistic magnetospheric electric and magnetic fields, greatly reducing computer simulation times. The method works for particles having arbitrary charge, energy, or pitch angle but which conserve the first two adiabatic invariants. We also apply an efficient method of classifying drift orbits, which greatly simplifies the task of identifying the last closed drift path or other drift boundaries. Finally, we calculate the time-independent evolution of the bounce-averaged phase space density along convective drift orbits. With these three tools, convective evolution of the particle distribution from the tail can now be described quantitatively, an essential step in understanding the production of unstable distributions in the magnetosphere. One can also categorize topologically different drift orbits, which is necessary to understand the unique particle signatures of the convecting plasma such as Alfvén layers and the plasmapause. These signatures can then be used to extract the electric and magnetic fields or to test the validity of the model fields. The method is particularly appropriate for particles in the energy range 0.01<E<100 keV, which are influenced by both electric and magnetic fields, and for time periods without invariant destroying waves.

1 INTRODUCTION

A major problem hindering the data modeling efforts to describe particle motion in the magnetosphere has been the highly computer intensive algorithms needed. Particle convection in a realistic magnetosphere has generally been analyzed with a numerical method that integrates the forces acting on the particle with time, essentially a Lagrangian approach, [e.g., *Ejiri et al.*, 1978]. These techniques can analyze a few (< 1000) particles for a few (< 10) hours, but are not efficient enough (even for fast computers) to follow the evolution of an entire phase space distribution over long time periods. A Hamiltonian energy conservation approach can produce a more efficient, and therefore more powerful algorithm for tracing the entire time evolution of the phase space distribution. Although the method has been known since the early days of magnetospheric research, [e.g., *Roederer*, 1970], it has generally been applied only to the equatorially trapped, 90° pitch angle particles. *Taylor and Hones* [1965] show how non-equatorial pitch angles can be analyzed, *McIlwain* [1974] showed how global fields can be extracted from geosynchronous satellite data with the method and *Whipple* [1978] developed a coordinate transformation that greatly simplifies both tasks.

A second problem, even when particle trajectories are given, is classifying the types of drift orbits and identifying the boundaries between classes. For a simple dipole magnetic field and a Volland-Stern [*Volland*, 1973, *Stern*, 1973] electric field, analytic expressions can be derived that, for example, specify the stagnation point of the plasmapause. It was this identification that permitted *Maynard and Chen* [1975] to calculate a K_p dependent electric field from particle signatures. A more realistic magnetosphere, however, does not lend itself to analytic expressions, making the boundaries much harder to identify and correlate with data. We show that not only does the conservation of energy method calculate trajectories rapidly, it also provides a very efficient classification scheme that can automate the search for topological boundaries.

The third problem arises from the wide gap between analytic, fluid MHD theories and the models which trace discrete particle trajectories. Without the relevant distribution function, one cannot calculate growth rates and wave-particle interactions self-consistently. Two common, but computationally intensive methods for estimating the distribution function either used vast numbers of particles to construct the moments numerically, or extrapolated distributions from a select subset of particle energies. An alternative fluid approach [e.g., *Northrop and Teller*, 1960] calculates the bounce averaged phase space density along the drift trajectories, which opens up the data to the powerful tools of global MHD analysis. The fluid description can be extended to include the effects of diffusion and loss and even time-dependence. Thus one can begin to create quantitative models of the entire convecting plasma without being restricted to discontinuities at topological boundaries.

We develop three tools that address each of these problems, and demonstrate them by displaying the effect of pitch angle on convecting ion trajectories in realistic magnetic and electric fields, which, to our knowledge, has not been done before.

2 THEORY

The first two tools are carefully described by Whipple, so we give a brief summary of the Hamiltonian method and classification scheme. If a charged particle conserves the first two adiabatic invariants, it also conserves energy, since the first invariant, $\mu = E_\perp/B$ is proportional to the perpendicular kinetic energy (K.E.), and the second invari-

Paper number 93GL00835
0094-8534/93/93GL-00835$03.00

ant, $J = m \oint v_{\|} ds$, is proportional to the parallel velocity. Implicit in the use of the first two invariants is an average over the gyro and bounce motion of particle. The key idea is that particle drift motion must conserve energy so that a drift trajectory must be a contour of constant total energy, and calculation of these contours is much faster and more efficient than integration of forces. If there are no inductive electric fields due to a changing magnetic field, $\partial B/\partial t = 0$, then we can express the electric field as the gradient of a scalar, U. Assuming that the drift speed is insignificant compared to gyration, we can write the total energy as, $W = KE + PE = mv^2/2 + qU = \mu B_m + qU$, where $B_m(K)$ is the magnetic field magnitude at the mirror point. We label particles by their μ and K values, where $K = J/\sqrt{2m\mu} = 4\int_0^m \sqrt{B_m - B(s)}ds$. So then, rather than considering drift motion only in the equatorial plane, we calculate the iso-energy contours on a mirror point K-surface, and then map to the equatorial plane.

Whipple showed that one can greatly simplify the classification of drift orbits by a coordinate transformation which relies on the conservation of energy; i.e., since $dW/dt = 0 = d(\mu B_m)/dt + d(qU)/dt$, then

$$\frac{\partial U}{\partial B_m(K)} = \frac{-\mu}{q} \qquad (1)$$

Which says that in UB(K) space, particle trajectories are straight lines whose slope is proportional to $-\mu/q$. For a simple dipole magnetic field with a Volland-Stern electric field (Figure 1), the mapping from real space to UB(K) space is double valued. However, this can be resolved by splitting the magnetosphere into night and day halves, the boundary being the line at which contours of constant B and U are tangent. In the night half of the magnetosphere the particles convect toward higher B (earthward), while on the day side particles convect toward lower B (anti-earthward), easily distinguishing the two populations. When a particle orbit crosses a tangency line in real space, it reverses direction in UB(K) space so that these tangency lines are also limits of motion in UB(K) space. The ionosphere of the earth and the magnetopause complete the bounding of particle motion in UB(K) space.

With this mapping, topological boundaries become simple geometrical constructions involving slopes and tangents, which can be easily automated and calculated to any level of precision. For example, the plasmapause is the last closed drift orbit for a zero energy ion. This translates to a horizontal line in UB(K) space that is tangent to the peak of the lower bounding tangency curve. Likewise the Alfvén layer for any energy is found by picking an energy (slope) that intersects the tail and making it tangent to the appropriate bounding curve such that it maximally penetrates into the magnetosphere.

One must recalculate this mapping for each value of K, or equatorial pitch angle desired. In general the tangency curves can be very different, even changing the topology of the drift boundaries in UB(K) space. These bounce averaged drift orbits are then mapped in real space along the field lines to the equatorial plane to compare trajectories of differing K (Figure 2).

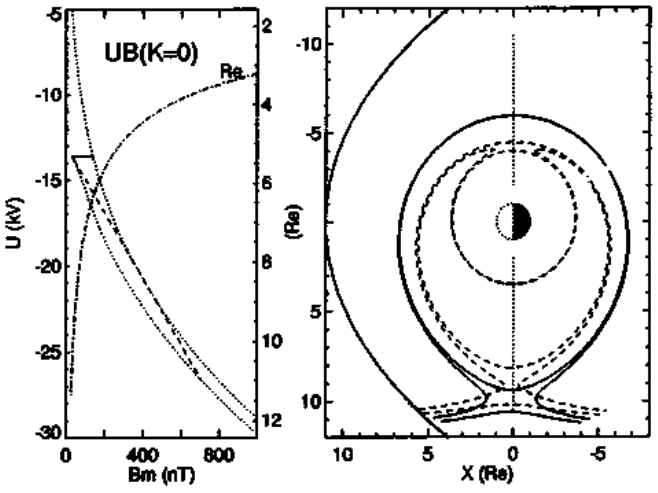

Fig. 1: An equatorial cut in the X-Y plane to UB(K) mapping for a dipole magnetic field + Volland-Stern [*Volland*, 1973, *Stern*, 1973] shielded electric field appropriate for K_p=0 [*Maynard and Chen*, 1975]. Lines of tangency between contours of constant B and U are shown dotted. Dash-dotted line converts B_m to radial distance with right hand scale. The plasmapause, the last closed 0.0 eV/nT trajectory, is bracketed by solid lines. The open drift trajectory that penetrates most deeply into the magnetosphere is bracketed by dashed lines. With a slope of 19.2 eV/nT, it follows a banana orbit but only crosses a tangency line once, at dusk close to the earth.

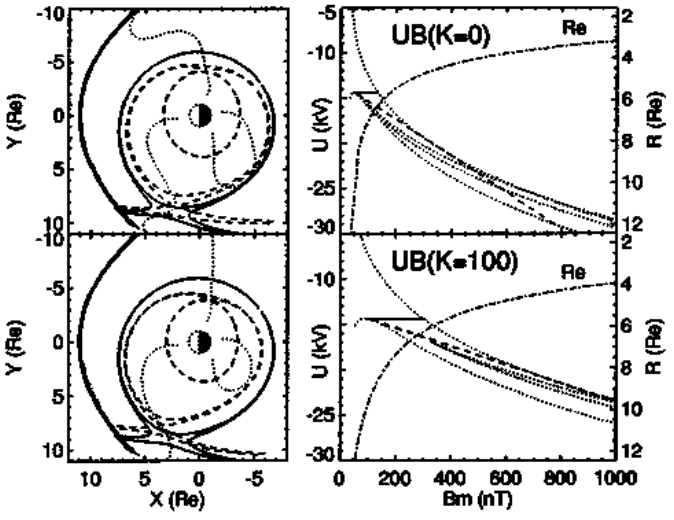

Fig. 2: Equatorial X-Y to UB(K) mapping for realistic Olson-Pfitzer [*Olson et al.*, 1979] magnetic field and Volland-Stern (K_p=0) + ionospheric dynamo [*Richmond et al.*, 1980] electric fields. Top panels calculated for 90° pitchangles, K=0; bottom panels for K=100. The extra loop in X-Y tangency curves generated by a quadrupolar ionospheric field becomes a topological pleat in UB(K) space. Trajectories labelled similarly as previous figure. Dashed trajectory has a slope of 10.2 eV/nT in top panels, 20.2 eV/nT in bottom panels.

In the guiding center approximation, we know [eq. 35, *Northrop and Teller,* 1960] that the phase space density

$$Q(\alpha, \beta, J, \mu) = \pi f(\vec{r}, \vec{v})/m^2 \quad (2)$$

is conserved along the bounce-averaged convection trajectory, where α, β are the Euler potentials for labeling field lines, μ, J are the first and second invariants, and f is the standard phase space density. An equivalent description in terms of the particle total energy is [eq. 41, *Northrop and Teller,* 1960],

$$n(\vec{r}, W, \mu) = 2BQ/v_{\|} \quad (3)$$

where W is the total energy defined above, $v_{\|}$ is the parallel velocity, and n is the number of particles in d^3r at a given value of W, μ.

3 Algorithms and Results

To carry out this method for any K or equatorial pitch angle, we need an algorithm for calculating the functional dependence of $B_m(K)$ on K. We do this numerically, (Figure 3), first mapping the field line from the equator to the ionosphere, here showing several longitudes collapsed into one display. We numerically integrate these B(s) curves to obtain the second adiabatic invariant K(s). Note that on the day side, there are field lines which do not have a minimum at the equator, and thus K is undefined (imaginary) over some range of s. *Northrop and Teller* [1960] discuss this phenomenon, and like them, we find a generalized form of K defined as the sum of all non-imaginary K's along a field line. With that definition, we calculate K from the minimum, either at the equator or elsewhere, to get K(s). With these two quantities, we can now calculate $B_m(K)$ as a polynomial expression, plotted in the final panel. We use 10th degree polynomials and arrive at an expression with less than 3% maximum deviation. Note that this is just an automated way of carrying out the Taylor and Hones graphical method, which we independently derived.

This part of the algorithm is the most time consuming, taking 5 hours on a SUN IPC for solving a 100 x 100 grid of the equatorial plane and using 200 integration steps along a field line. Once the polynomials are initialized, calculating a total energy for arbitrary K and μ, which gives simultaneously every spatially distinct trajectory in the equatorial plane, required only 30 seconds, or only 3 seconds if μ alone changes. This is to be contrasted with 3 minutes per single particle trace using a predictor-corrector method to time-integrate the forces.

Now that we have a realistic B(K) mapping, we also need to make U more realistic as well. *Pinto et al.* [1987] showed that drift trajectories would be greatly influenced by the ionospheric dynamo electric field [*Richmond et al.,* 1980]. This dynamo field strengthens convection at low L-shells and compensates for the Volland-Stern shielding. However, the field is quadrupolar and topologically different from the dipolar Volland-Stern field, so that (Figure 2) in real space the tangent lines form a loop at low altitudes. When mapped into UB(K) space, the loop becomes a pleat, but only in the night half of the magnetosphere.

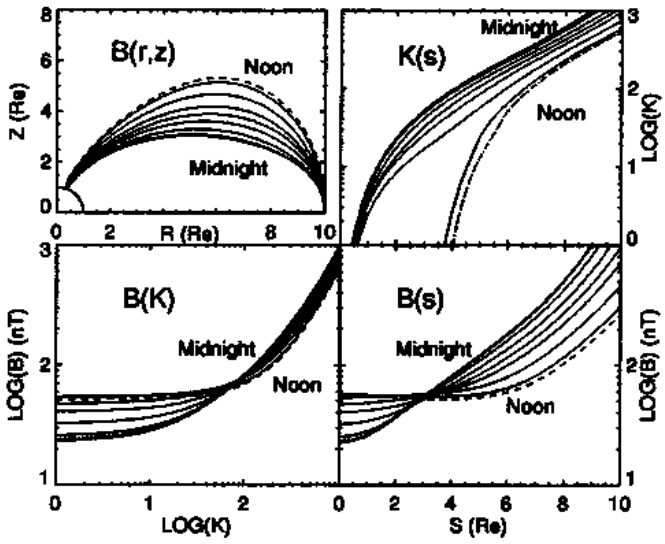

Fig. 3: a) Fieldlines traced from equatorial plane at 10 Re with longitude varying from midnight to noon in 20° increments; b) K(s) for fieldlines at 10 Re; c) B_m(K), which is well defined for all fieldlines; and d) B(s) for fieldlines at 10 Re with an off equatorial minimum in the noon fieldline.

Since this is the first time trajectories have been shown for these realistic fields, we plot some examples in Figure 4. In panel (a), we see that for K=0 or 90° equatorial pitch angles at a magnetic moment of 0.01 keV/nT, there are closed drift trajectories that do not encircle the earth [e.g., *Chen,* 1970], called "banana" orbits after tokomak usage [*Strangeway and Johnson,* 1984]. In UB(K) space, these orbits are straight lines that nest in a concavity of the lower tangency curves. Note that the extra loop supports a new class of banana orbits; however these banana orbits are inside normal, earth encircling trapped orbits, and thus have no access to the open drift trajectories from the tail. In panel (b), we see that for K=100, the banana orbits merge and appear outside the normal trapped orbit region. This allows them to be readily filled by diffusion or Coulomb drag effects. More importantly, there exists an open drift orbit threading between the normal closed orbits and the banana orbits. Because of the large value of B at low altitudes, convecting tail particles on this open drift trajectory become more pancake-like as the pitch angle rotates toward 90°, panel (c), and equatorial $n(\vec{r}_{eq}, W, \mu)$ increases. Panel (d) plots the change in $B_{eq}/\sqrt{\mu(B_m - B_{eq})}$, which is directly proportional to the change in $n(\vec{r}_{eq}, W, \mu)$. Since this orbit is open to the tail, unlike its near neighbors, it alone experiences an order of magnitude increase in $n(\vec{r}_{eq}, W, \mu)$ for some specific range of W, μ. This mechanism can explain the peaks seen in this vicinity by ISEE-1, [*Williams and Frank,* 1984, *Sheldon,* 1993].

Acknowledgments. This work was supported by grant NAG-5-1558. We benefitted from many helpful discussions with M. Collier, S. Christon, T. Eastman, M. Greenspan, T. Birmingham and especially, T. Northrop. We especially thank the referee who brought the Taylor and Hones article to our attention and for many helpful comments.

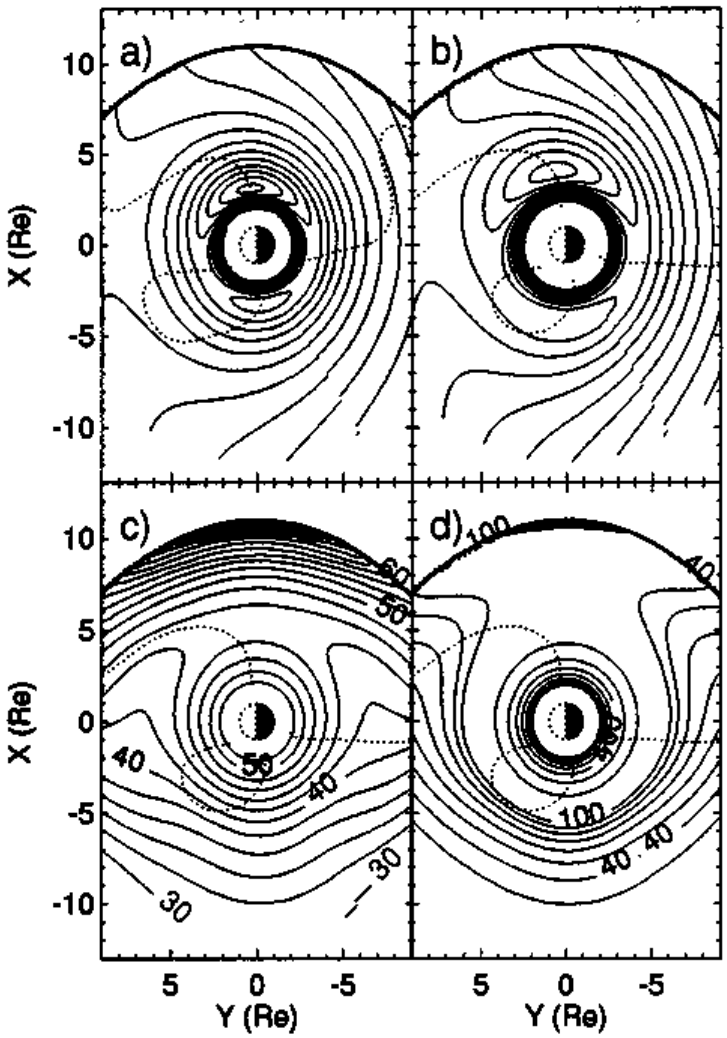

Fig. 4: a) X-Y space trajectories for μ = 0.01 keV/nT, K=0; b) X-Y space trajectories for μ = 0.01 keV/nT, K=100; c) K=100 Equatorial pitch angles α, contours every 2°; and, d) $B_m(K)/\sqrt{\mu(B_m(K)-B_{eq})}$ for μ=0.01 keV/nT, K=100.

References

Chen, A. J., Penetration of low-energy protons deep into the magnetosphere, *J. Geophys. Res.*, *75*, 2458–2467, 1970.

Ejiri, M., R. A. Hoffman, and P. H. Smith, The convection electric field model for the magnetosphere based on Explorer 45 observations, *J. Geophys. Res.*, *83*, 4811–4815, 1978.

Maynard, N. C. and A. J. Chen, Isolated cold plasma regions: observations and their relation to possible production mechanisms, *J. Geophys. Res.*, *80*, 1009, 1975.

McIlwain, C. E., Substorm injection boundaries, in *Magnetospheric Physics*, edited by B. M. McCormac, pp. 143–154, D. Reidel Publishing Co., Dordrecht-Holland, 1974.

Northrop, T. G. and E. Teller, Stability of the adiabatic motion of charged particles in the earth's field, *Phys. Rev.*, *117*, 215, 1960.

Olson, W. P., K. A. Pfitzer, and G. J. Mroz, Modeling the magnetospheric magnetic field, in *Quantitative Modeling of Magnetospheric Processes, Geophys. Monogr. Ser. vol. 21*, edited by W. P. Olson, pp. 77–85, American Geophysical Union, Washington D.C., 1979.

Pinto, Jr., O., O. Mendes, Jr., and W. D. Gonzalez, Dynamics of equatorial low-energy particles inside the plasmasphere during magnetically quiet periods, *J. Geophys. Res.*, *92*, 10130–10132, 1987.

Richmond, A. D., M. Blanc, B. A. Emery, R. H. Wand, B. G. Fejer, R. F. Woodman, S. Ganguly, P. Amayenc, R. A. Behnke, C. Calderon, and J. V. Evans, An empirical model of quiet-day ionospheric electric fields at middle and low latitudes, *J. Geophys. Res.*, *85*, 4658–4664, 1980.

Roederer, J. G., *Dynamics of Geomagnetically Trapped Radiation, Physics and Chemistry in Space, Volume 2*, Springer-Verlag, New York, 1970.

Sheldon, R. B., Plasmasheet convection into the inner magnetosphere during quiet conditions, *Adv. Space Res.*, in press 1993.

Stern, D. P., A study of the electric field in an open magnetospheric model, *J. Geophys. Res.*, *78*, 7292–7305, 1973.

Strangeway, R. J. and R. G. Johnson, Energetic ion mass composition as observed at near-geosynchronous and low altitudes during the storm period of February 21 and 22, 1979, *J. Geophys. Res.*, *89*, 8919–8939, 1984.

Taylor, H. E. and E. W. Hones, Jr., Adiabatic motion of auroral particles in a model of the electric and magnetic fields surrounding the earth, *J. Geophys. Res.*, *70*, 3605–3628, 1965.

Volland, H., A semiempirical model of large-scale magnetospheric electric fields, *J. Geophys. Res.*, *78*, 171–180, 1973.

Whipple, Jr., E. C., (U,B,K) coordinates: a natural system for studying magnetospheric convection, *J. Geophys. Res.*, *83*, 4318–4326, 1978.

Williams, D. J. and L. A. Frank, Intense low-energy ion populations at low equatorial altitudes, *J. Geophys. Res.*, *89*, 3903–3911, 1984.

J. D. Gaffey Jr., 10105 Frederick Av., Kensington, MD 20895

R. B. Sheldon, Physikalisches Institut, Universitaet Bern, Sidlerstrasse 5, CH-3012 Bern, Switzerland

(Received November 6, 1992;
revised January 28, 1993;
accepted February 24, 1993.)